Heat flux from the surface in the process of the rupture of a thin liquid film by an electric field ⊘

A. L. Kupershtokh ✉ ⓘ ; D. A. Medvedev ⓘ ; A. V. Alyanov ⓘ

Check for updates

CrossMark

View Online

Export Citation

Articles You May Be Interested In

Completing the dark matter solutions in degenerate Kaluza-Klein theory

J. Math. Phys. (April 2019)

Gibbs measures based on 1d (an)harmonic oscillators as mean-field limits

J. Math. Phys. (April 2018)

An upper diameter bound for compact Ricci solitons with application to the Hitchin–Thorpe inequality. II

J. Math. Phys. (April 2018)

Physics of Fluids

AIP Publishing

Heat flux from the surface in the process of the rupture of a thin liquid film by an electric field

View Online   Export Citation   CrossMark

A. L. Kupershtokh,[a] (iD) D. A. Medvedev, (iD) and A. V. Alyanov (iD)

AFFILIATIONS

Lavrentyev Institute of Hydrodynamics of SB RAS, 630090 Novosibirsk, Russia

[a] Author to whom correspondence should be addressed: skn@hydro.nsc.ru

ABSTRACT

In this article, the cooling of a solid surface by an evaporating film of a dielectric liquid and the influence of an electric field on this process are studied. The mesoscopic lattice Boltzmann method is applied to simulate the fluid flow with phase transitions and the heat transfer. The cases without electric field, with initially uniform electric displacement field, and with non-uniform electric field are considered. A uniform field enhances the cooling slightly. Non-uniform field leads to the rupture of the film. In this case, the local heat flux in local regions increases significantly when the film becomes thin and effectively evaporates. After the rupture of the film, the heat flux from a dry spot decreases abruptly. The formation of a dry spot can be prevented by switching off the electric field before the film rupture. Thus, we demonstrate the possibility of enhanced cooling of local regions at a surface using pulses of non-uniform electric field acting on a thin film of dielectric liquid placed at the surface. If the inflow of liquid to the film could be provided, it is in principle possible to realize a periodic process of application of voltage pulses to electrodes and to enhance the cooling of surface by the evaporation of a film of dielectric liquid.

I. INTRODUCTION

In recent years, a new scientific direction is developed, controlling the movement of small volumes of dielectric and conducting liquids using, in particular, electric fields. On this basis, attempts are being made to create microelectromechanical devices (micro-fluidic devices) for the purpose of moving, mixing, and separating liquids in chemical, medical, and biotechnologies using the so-called laboratories on chips (lab-on-a-chip).

The rupture of thin liquid films can occur in many industrial applications related to dispersed and colloidal systems and other technical phenomena. Experimental and theoretical studies on thermocapillary instability and rupture of thin liquid films on a heated surface were presented in Refs. 1 and 2.

Electric field is one of the suitable instruments for controlling the shape of liquid droplets and their motion along a solid surface[3–10] as well as for changing the shape of the surface of dielectric liquid films.[9–13]

Electrostatically induced pumping in microchannels and patterning under the action of an externally applied non-uniform electric field were described in Refs. 12 and 13. In Ref. 12, numerical calculations of the deformation of the free surface of thin films in an electric field between horizontal electrodes were carried out. Protrusions were specially created on the upper electrode so that the vertical electric field

became non-uniform. The growth of prominences reduces the air gap between the film and the upper electrode, which enhances the electric field and accelerates their evolution. The development of electrohydrodynamic instability and the controlled development of structures are shown.

In Ref. 13, a liquid dielectric film is located above the lower plane, in which a pair of electrodes is mounted, and an electric field is created between them. The deformation of the film surface is experimentally shown. Obviously, the liquid is drawn into the region of high electric field and rises above the initial level.

In the method proposed by us,[10,14,15] a non-uniform electric field is created by non-conductive insets in segmented lower electrodes. In this case, on the contrary, the dielectric liquid is drawn from the area above the non-conductive insert and is pulled into the region with a higher field magnitude over the conductive electrodes. The thinning of the film occurs, and its rupture is possible.

In Refs. 14 and 15, it was shown by the three-dimensional computer simulation that the process of perforation depends on the initial field magnitude, the film thickness, the shape and the size of non-conductive insets, and the value of surface tension. Hence, influence of these factors was combined in the modified electric Bond number.[14,15] However, heat fluxes were not calculated in these works.

05 October 2023 02:40:56

Liquid films and droplets are widely used for the cooling of heated surfaces. This method is efficient because the surface is cooled intensely at the evaporation due to the absorption of the latent heat of evaporation. One of the methods to evacuate the produced vapor is used in heat pipes where the vapor condenses at a special cold section. It is commonly assumed that the cooling of hot surfaces by the evaporation of liquid films and droplets is more effective when many contact lines are present.[16–20]

It was shown in Ref. 21 that the total heat flux did not always increase after the rupture because of the formation of dry spots at the surface and decreasing heat flux to the gas phase.

In the present work, we investigate the possibility of intensification of the heat removal from the heated surface during the process of the deformation of a dielectric liquid film before its rupture. Two-dimensional problems of evaporation of a liquid film from the surface of a heated solid or segmented lower electrode and the condensation at a cooled upper electrode are considered. The lattice Boltzmann method is used to simulate the fluid dynamics[22,23] and the convective heat transfer.[24]

II. METHODS

A. Lattice Boltzmann method for fluid flow

In this method, the fluid dynamics is simulated by means of pseudoparticles (also called one-particle distribution functions) f_k, which can move along the links of a regular spatial lattice and undergo collisions in its nodes. The vectors of allowed velocities $c_k, k = 0, \ldots, n$ and the time step Δt are chosen so that their products are equal to the lattice vectors $e_k = c_k \Delta t$. Frequently used lattice arrangements are D1Q3 (one-dimensional space with three velocity vectors), D2Q9 (2D space, nine lattice vectors), and D3Q19 (three dimensions, 19 velocity vectors). The possible values of velocity in last two cases are $0, h/\Delta t$, and $\sqrt{2}h/\Delta t$.

The distribution functions evolve according to the following lattice Boltzmann equation:

$$f_k(\mathbf{x} + \mathbf{e}_k, t + \Delta t) = f_k(\mathbf{x}, t) + \Omega_k(\{f_k\}) + \Delta f_k. \quad (1)$$

There is a term corresponding to the free motion of pseudoparticles, the discrete analogue of the Boltzmann collision integral, and the change of f_k due to the action of volume forces.

The collision operator Ω_k is often used in the form of BGK (Bhatnagar–Gross–Krook),[25] which has the form of the relaxation to local equilibrium values f_k^{eq} with a single relaxation time,

$$\Omega_k = (f_k^{eq}(\rho, \mathbf{u}) - f_k(\mathbf{x}, t))/\tau. \quad (2)$$

The fluid density ρ and velocity $\mathbf{u}$ are calculated from the distribution functions f_k as

$$\rho = \sum_{k=0}^{n} f_k, \quad \rho\mathbf{u} = \sum_{k=0}^{n} f_k \mathbf{c}_k. \quad (3)$$

The truncated Maxwell–Boltzmann formula is commonly used for the equilibrium distribution functions f_k^{eq}[26]

$$f_k^{eq} = \rho w_k \left(1 + \frac{\mathbf{c}_k \cdot \mathbf{u}}{\theta} + \frac{(\mathbf{c}_k \cdot \mathbf{u})^2}{2\theta^2} - \frac{u^2}{2\theta}\right). \quad (4)$$

Here, $\theta = h^2/(3\Delta t^2)$.

Change of the distribution functions Δf_k due to the action of body forces (internal and external) is calculated using the exact difference method (EDM) first proposed in Ref. 27. It is described in more detail in Ref. 28. The values of the fluid velocity before $\mathbf{u}$ and after the action of force $\mathbf{u} + \Delta\mathbf{u}$ are used,

$$\Delta f_k = f_k^{eq}(\rho, \mathbf{u} + \Delta\mathbf{u}) - f_k^{eq}(\rho, \mathbf{u}), \quad (5)$$

where $\Delta\mathbf{u} = \mathbf{F}\Delta t/\rho$. Compared to other methods, EDM is Galilean invariant. This method is widely used and included in international computer simulation packages: LBsoft, OpenLB, and DL-MESO.[29–31]

The physical fluid velocity in this case is[32]

$$\mathbf{u}^* = \mathbf{u} + \Delta\mathbf{u}/2. \quad (6)$$

For simulating phase transition liquid–vapor, the method of pseudopotential is used.[33] The force acting at the fluid in a node is expressed as the gradient of the pseudopotential $\mathbf{F} = -\nabla U$, where $U = P(\rho, T) - \rho\theta$ is defined by the equation of state $P(\rho, T)$. We follow the approach of[23,34]

$$\mathbf{F} = 2A\nabla(\Phi^2) + (1 - 2A)2\Phi\nabla\Phi, \quad \Phi = \sqrt{-U}. \quad (7)$$

The free parameter A allows one to adjust equilibrium liquid and vapor values for the best agreement with the theoretical coexistence curve.

Van der Waals equation of state is used, which is written for one mole as

$$P = \frac{RT}{V - b} - \frac{a}{V^2}. \quad (8)$$

Using non-dimensional variables $\tilde{P} = P/P_{cr}, \tilde{T} = T/T_{cr}, \tilde{\rho} = \rho/\rho_{cr}$ ($P_{cr}, T_{cr}, \rho_{cr}$ are the critical values), Eq. (8) takes the following form:

$$\tilde{P} = \frac{8\tilde{\rho}\tilde{T}}{3 - \tilde{\rho}} - 3\tilde{\rho}^2. \quad (9)$$

For this equation of state, the best choice of the parameter is $A = -0.152$.[23]

B. Lattice Boltzmann method for heat transfer

To simulate the heat transfer, we use an additional set of distribution function g_k. The internal energy density E is expressed as

$$E = \sum_{k=0}^{n} g_k. \quad (10)$$

Variables g_k evolve according to the equation similar to Eq. (1),

$$g_k(\mathbf{x} + \mathbf{e}_k, t + \Delta t) = g_k(\mathbf{x}, t) + (g_k^{eq} - g_k)/\tau_E + \Delta g_k. \quad (11)$$

The term Δg_k consists of two parts $\Delta g_k = \Delta g_k^{(1)} + \Delta g_k^{(2)}$. The first term

$$\Delta g_k^{(1)} = g_k^{eq}(E, \mathbf{u} + \Delta\mathbf{u}) - g_k^{eq}(E, \mathbf{u}) \quad (12)$$

prevents the parasitic heat diffusion across phase boundaries, and the second one corresponds to the change of internal energy,

$$\Delta g_k^{(2)} = g_k \frac{\Delta E}{E}. \quad (13)$$

Here, $\Delta E = \Delta E_P + \Delta E_C + \Delta E_Q$ takes into account all heat sources as follows: the pressure work

$$\Delta E_P = -P \operatorname{div}(\mathbf{u}^*)\Delta t, \qquad (14)$$

the conductive heat flux

$$\Delta E_C = \operatorname{div}(\operatorname{grad}(\lambda T))\Delta t, \qquad (15)$$

and the release or absorption of the latent heat of phase transition

$$\Delta E_Q = \frac{\rho_L Q(T)}{\rho_2 - \rho_1}\frac{d\rho}{dt}\Delta t = -\frac{\rho_L Q(T)}{\rho_2 - \rho_1}\rho \operatorname{div}(\mathbf{u}^*)\Delta t. \qquad (16)$$

The coefficient λ in Eq. (15) is the thermal conductivity of the fluid, and Q in Eq. (16) is the latent heat of evaporation per unit mass. For more detailed description, the reader is referred to the paper.[24]

For the van der Waals equation of state (8), the internal energy for one mole of fluid is equal to[35]

$$E_M = E_{\text{IG}} - a/V, \qquad (17)$$

where $E_{\text{IG}} = C_v T$ is the internal energy of ideal gas, and C_v is the specific heat at fixed volume. Hence, the latent heat of evaporation per unit mass is

$$Q = a(\rho_L - \rho_V), \qquad (18)$$

where ρ_L and ρ_V are the equilibrium densities of liquid and vapor. Using Eq. (16) and taking $\rho_2 = \rho_L, \rho_1 = \rho_V$, we obtain finally

$$\Delta E_Q = -a\rho_L \rho \operatorname{div}(\mathbf{u}^*)\Delta t. \qquad (19)$$

In non-dimensional values, Eq. (19) takes the following form:

$$\Delta E_Q = -3\tilde{\rho}_L \tilde{\rho} \operatorname{div}(\mathbf{u}^*)\Delta t. \qquad (20)$$

The term $\operatorname{div}(\mathbf{u}^*)$ is calculated using central finite differences, as well as the change of energy due to conductive transport [Eq. (15)].

C. Boundary conditions

For fluid, well-known bounce-back rule[36] is applied at rigid walls, which produces impermeability and no-slip boundary conditions. To simulate the degree of a surface wettability, we use the method proposed in Refs. 14, 15, 37, and 38. For this purpose, it is necessary to take into account the forces of interaction between the liquid and the substrate. In two-dimensional case, the force acting on a node of fluid adjacent to the wall is calculated using three nearest solid nodes as

$$\mathbf{F}(\mathbf{x}) = \Phi(\mathbf{x}) \sum_{j=1}^{3} w_j B(\mathbf{x} + \mathbf{e}_j)\Phi_{\text{solid}}(\mathbf{x} + \mathbf{e}_j)\mathbf{e}_j. \qquad (21)$$

Here, Φ_{solid} is equal to the value of Φ in the nearest fluid node. The coefficient B controls the wettability of the surface and the contact angle. The value $B = 1$ results in the wetting angle of $90°$.

Unfortunately, for $B \neq 1$, this method leads to variations in fluid density near the surface,[14,15,37,38] which hampers the calculation of heat fluxes. To overcome this flaw, a new method was proposed in Ref. 21. There, the combination of neutral wetting in accordance with Eq. (21) at $B = 1$ and additional forces parallel to the surface was used. For a horizontal wall, the sum of these additional forces is given by the following formula:

$$\mathbf{F}_x(\mathbf{x}) = D\Phi(\mathbf{x}) \sum_{j=1}^{3} \Phi_{\text{solid}}(\mathbf{x} + \mathbf{e}_j)e_{jx}. \qquad (22)$$

The neutral wetting remains for $D = 0$. Values of $D < 0$ correspond to wettable surfaces, and $D > 0$ to non-wettable ones.

Distribution functions g_k for the internal energy in boundary nodes are set to equilibrium values corresponding to the prescribed temperature, zero velocity, and the density in the nearest fluid node.

Simulations are performed in a rectangular computational domain of the size $L_x \times L_y = 400 \times 200$. In all calculations, we assume $h = 1$ and $\Delta t = 1$, i.e., all sizes are measured in the lattice spacing h, and time is measured in the time steps Δt.

Gravitational force is acting downward along the Y axis, and the gravity acceleration is $g_y = 10^{-6}$. At the temperature $T = 0.7T_{cr}$, the value of gravitational Bond number $\text{Bo} = \rho g_y \delta^2 / \sigma$ is ≈ 0.06. Here, δ is the initial film thickness, and σ is the surface tension of liquid.

The heat flux from the lower heated surface is measured in calculation as

$$q = -\int_0^{L_x} \lambda \frac{\partial T}{\partial y}\, dx, \qquad (23)$$

where the values of the heat conductivity λ are taken in the layer of fluid adjacent to the surface.

III. SIMULATION RESULTS

A. Film evaporation without an electric field

Two-dimensional problem of the evaporation of a flat film of dielectric liquid placed at the surface of the lower flat electrode is solved. The initial film thickness is equal to $\delta = 30$. At the beginning, the temperature in the whole domain is set to $T = 0.7T_{cr}$, and the fluid velocity is zero everywhere. After the equilibration stage between the liquid film and the vapor (until $t = 5000$), the lower electrode is instantly heated to $T = 0.75T_{cr}$, and the upper one is cooled to $T = 0.6T_{cr}$.

Curves 1 and 2 (Fig. 1) show the time dependence of the heat flux from the electrode surface without an electric field. Calculations by the one-dimensional D1Q3 (curve 1) and two-dimensional D2Q9 (curve 2) models produce identical results. At the initial stage, the heating of the film occurs, and a quasi-steady evaporation regime is established.[21] Then, the film thickness decreases due to evaporation, leading to the gradual increase in the heat flux. Small oscillations decaying with time are causes by the reverberation of waves generated by the perturbations related to the instant switch-on of the heating at $t = 5000$.

B. Evaporation of film in initially uniform electric displacement field

Two-dimensional problem of the evaporation of a flat film of dielectric liquid placed at the surface of the lower flat electrode is solved. The initial film thickness is equal to $\delta = 30$. At $t = 12\,000$, constant voltage is applied between the electrodes producing the initially uniform electric displacement field $D_0 = \varepsilon_0 \varepsilon(y)E$, where E is the local electric field, and ε_0 is the electrostatic constant. The electric permittivity ε for non-polar liquids depends on the local fluid density ρ according to the Clausius–Mossotti formula,
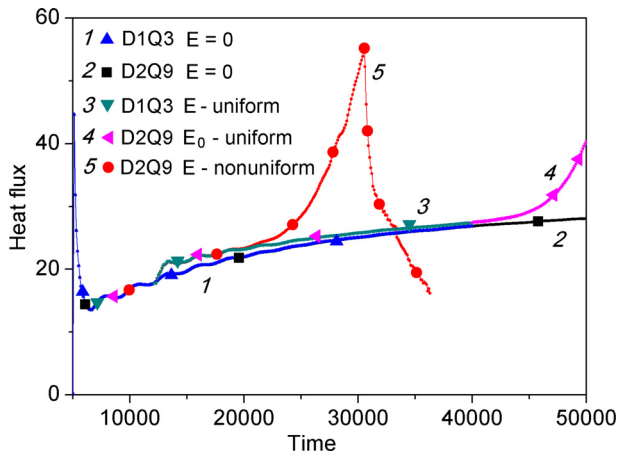
FIG. 1. Time dependence of the total heat flux from the electrode surface without an electric field (curves 1 and 2) and after the application of the initially uniform electric displacement field without non-conductive inset (curves 3 and 4). Curve 5 corresponds to the case of non-uniform electric field (with non-conductive inset). Curves 1 and 3—calculations of the heat flux by the one-dimensional D1Q3 model rescaled to $L_x = 400$. Curves 2, 4, and 5—two-dimensional calculations by the D2Q9 model. Electric bond number is equal to $Bo_E^* = 4.6$.

$$\varepsilon = 1 + \frac{3\alpha\tilde{\rho}}{1 - \alpha\tilde{\rho}}. \tag{24}$$

The value of $\alpha = 0.141$ is chosen so that the value of permittivity of liquid is $\varepsilon_l = 2.3$ at the initial temperature $T = 0.7T_{cr}$.

Electrostatic force **F** acting on a unit volume of dielectric fluid is defined by the following Helmholtz formula:[39]

$$\mathbf{F} = -\frac{\varepsilon_0 E^2}{2}\operatorname{grad}\varepsilon + \frac{\varepsilon_0}{2}\operatorname{grad}\left[E^2\rho\left(\frac{\partial\varepsilon}{\partial\rho}\right)_T\right]. \tag{25}$$

The electric field distribution is calculated at every time step by solving the Poisson's equations,

$$\operatorname{div}(\varepsilon\operatorname{grad}\varphi) = 0. \tag{26}$$

The electric potential at the upper solid electrode is constant $\varphi(x, L_y) = V$. At the conductive parts of the lower electrode, the potential is set to zero $\varphi(x, 0) = 0$. At the non-conductive inset, the normal component of the electric field is set to zero $E_y(x, 0) = \partial\varphi/\partial y = 0$. In two-dimensional calculations, the periodic boundary conditions are set at the side boundaries of the calculation domain $\varphi(L_x, y) = \varphi(0, y)$. The electric field is then calculated from the potential as $\mathbf{E} = -\operatorname{grad}\varphi$.

Time dependence of the heat flux from the electrode surface after the voltage application is shown in Fig. 1 for the one-dimensional D1Q3 (curve 3) and two-dimensional D2Q9 (curve 4) models. In such quasi-1D setting, the results are almost identical until $t \approx 40\,000$. After the switch-on of electric field, the heat flux increases slightly, since electrostatic forces accelerate the evaporation process of the film. In the 2D model, however, the film surface becomes unstable. The growth of prominences reduces the air gap between the film and the upper electrode, which strengthens the electrical field and accelerates the evolution. The heat flux increases due to the higher evaporation

rate at thinner parts of the film. For the geometry and other parameters used in the calculation, this occurs at $t > 40\,000$ (Fig. 1, curve 4).

C. Film rupture in a non-uniform electric field

Two-dimensional problem of the evaporation of a flat film of dielectric liquid placed at the surface of the lower flat electrode with a non-conductive inset of the size of $2R = 60$ is solved. The initial film thickness is equal to $\delta = 30$. At $t = 12\,000$, constant voltage is applied between the electrodes. The contact angle is equal to $\beta = 90°$, which corresponds to the neutral wetting.

The modified electric Bond number proposed in Refs. 14 and 15 depends on the film thickness δ and the characteristic size of the non-conductive inset R as

$$Bo_E^* = \varepsilon_0(\varepsilon_l - 1)E_0^2 R^2/(\delta\varepsilon_l\sigma). \tag{27}$$

Here, E_0 is the initial magnitude of the electric field above the surface of the film, and ε_l is the electric permittivity of liquid.

Under the action of a non-uniform electric field, the film becomes thinner in the region of non-conductive inset [Fig. 2(a), see also Refs. 10, 14, and 15]. This leads to the local increase in the temperature gradient, and the heat flux in this region increases [Fig. 2(b)] due to the rapid evaporation of this part of the film. The total heat flux also increases (curve 5 in Fig. 1). Just before the film rupture, the total heat flux increases more than twice. This will lead to enhanced local cooling of the surface.

After the rupture of the film ($t > 36\,000$), the heat flux from the dry spot drops significantly because the thermal conductivity of vapor is much lower than that of liquid (in our calculations, by the factor of 20). The total heat flux decreases accordingly (Fig. 1, curve 5). For comparison, the time dependence of the total heat flux is shown for one-dimensional problem (curve 3 in Fig. 1), where the deformation of the film is obviously absent, and the film thickness changes monotonously during the evaporation.
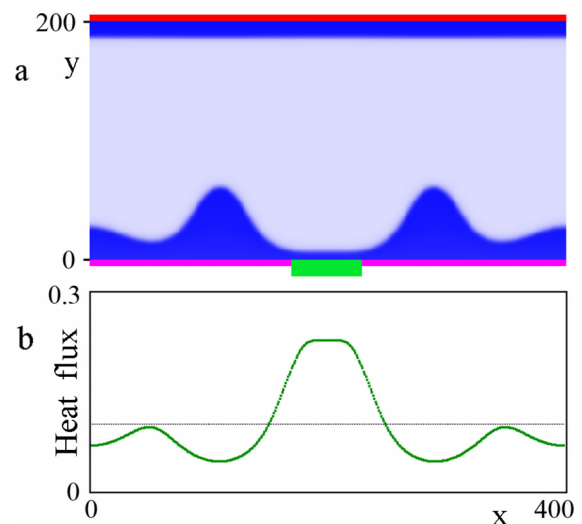
FIG. 2. (a) Deformation of the dielectric liquid film in the perforation process before the film rupture. (b) Distribution of the heat flux along the electrode surface. Time $t = 28\,000$. See Fig. 6 for multimedia view.

FIG. 3. Film rupture in a non-uniform electric field, compared with Fig. 2(a). Multimedia available online.

FIG. 5. Film behavior in a non-uniform electric field. Field switch-off before film rupture, compared with Fig. 4. Multimedia available online.

The value of the contact angle influences the flow of film after the breakup.[14,15] The growth of the dry spot is faster for non-wettable surfaces. Hence, the timescale for the variation of the heat flux depends on the contact angle. However, the overall development of the process does not change.

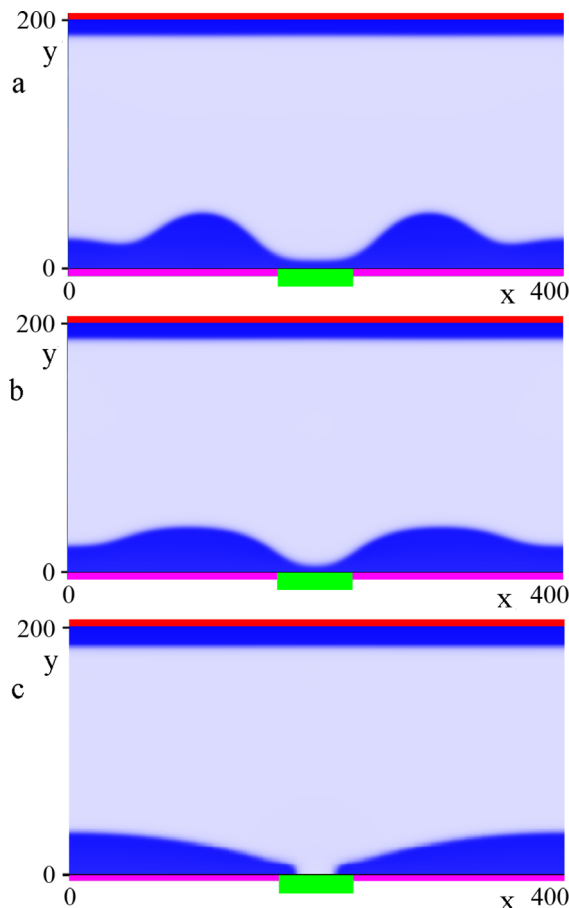The animation of the perforation process can be seen in Fig. 3 (Multimedia view).

Thus, it is possible to produce conditions for pulse cooling of local region at the surface by the perforation of thin films of dielectric liquid by the non-uniform electric field.

D. Heat flux during evaporation of film in non-uniform electric field. Field switch-off before film rupture

In order to avoid the film rupture and the formation of a dry spot, the electric field is switched off in the simulations before the rupture of the film at the time $t = 27\,000$. After this, the formation of the rupture stops [Fig. 4(a)], and liquid starts to flow into the region above the non-conductive inset [Fig. 4(b)].

The animation of the film behavior can be seen in Fig. 5 (Multimedia view).

When the electric field is switched off, the heat flux ceases growing and decreases for certain time (Fig. 6, curve 3). However, it is still higher than that in the absence of an electric field. During the evaporation of liquid from the surface, the total heat flux increases until the moment when the film breaks and a dry spot appears at the surface at $t \approx 51\,000$ [Fig. 4(c)].
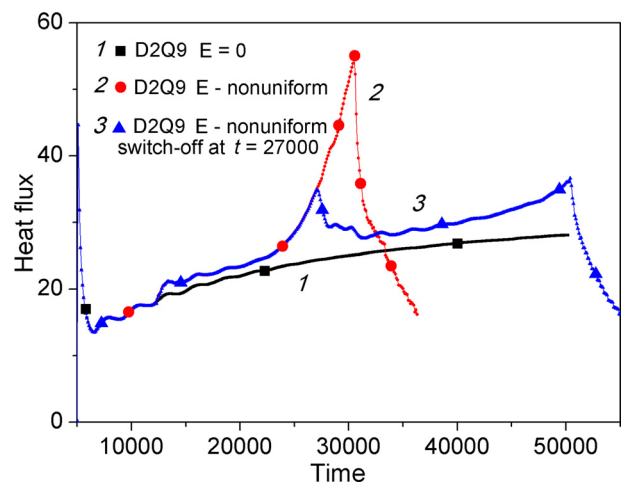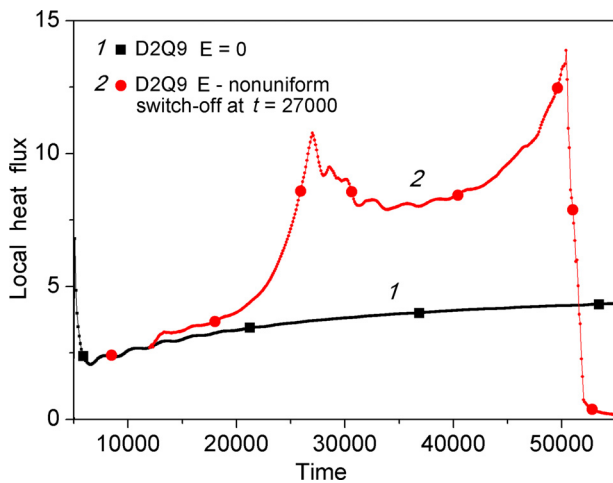

FIG. 4. Shape of the film surface after the switch-off of the electric field. Time is $t = 28\,000$ (a), $29\,000$ (b), and $51\,250$ (c).

FIG. 6. Time dependence of the total heat flux from the electrode surface without electric field (curve 1), and after the application of the non-uniform electric field at the time $t = 12\,000$ (curves 2 and 3). Curve 3 corresponds to the field switch-off at $t = 27\,000$.

FIG. 7. Time dependence of the local heat flux from the surface of non-conductive inset without electric field (curve 1) and with application of voltage at $12\,000 < t < 27\,000$ (curve 2).

Figure 7 shows the heat flux in local region (from the non-conductive inset). Curve 1 presents the local heat flux in the case without electric field. Curve 2 shows the local heat flux when the voltage is applied at the time interval $12\,000 < t < 27\,000$. The heat removal from the non-conductive inset increases almost twice until the moment of the film rupture and the appearance of a dry spot in this region ($t \approx 50\,000$). It is, therefore, possible to produce conditions for pulse cooling of local region at the surface by the perforation of thin films of dielectric liquid by the non-uniform electric field.

IV. CONCLUSION

We study the cooling of a solid surface by an evaporating film of dielectric liquid and the influence of an electric field on this process. The evaporation of a thin film of dielectric liquid is effective for enhancing the heat flux from a hot surface. A uniform electric field enhances cooling slightly, since electrostatic forces accelerate the evaporation of the film. Moreover, this process eventually leads to instability of the interface and to more intensive evaporation of thinner parts of the film. It is found that non-uniform electric field can be used for fast cooling of a local region of the surface. A non-uniform electric field can be created using non-conductive insets in segmented electrodes. However, the appearance of dry spots after film ruptures prevents the heat flux from these regions because the thermal conductivity of vapor over the hot surface is much lower than that of liquid.

For comparison of the results of different works, non-dimensional similarity criteria are useful. In our case, the relevant one is the electric Bond number (27), introduced in Ref. 14. At temperature $\tilde{T} = 0.7$, density $\tilde{\rho} \approx 0.32$, permeability $\varepsilon = 2.5$, surface tension $\sigma = 0.02$ J/m^2, film thickness $\delta = 1$ mm, and dielectric inset size $2R = 4$ mm, the electric Bond number equal to $\mathrm{Bo}_E^* \approx 2.4$ corresponds to the electric field strength of $E_0 \approx 15$ kV/cm. The listed parameters are close to those of the dielectric liquids PDMS (polydimethylsiloxane).

We demonstrate the possibility of enhanced cooling of local regions on the surface using short pulses of non-uniform electric field acting on the thin film of dielectric liquid. If the inflow of liquid to the

film could be provided, then, in principle, it is possible to realize a periodic process of applying voltage pulses to the electrodes and to enhance the surface cooling due to film evaporation for a long time.

AUTHOR DECLARATIONS
Conflict of Interest

The authors have no conflicts to disclose.

Author Contributions

Alexander L. Kupershtokh: Conceptualization (equal); Funding acquisition (lead); Investigation (equal); Methodology (equal); Software (equal); Validation (equal); Visualization (equal); Writing – original draft (equal); Writing – review & editing (equal). **Dmitry Medvedev:** Conceptualization (equal); Investigation (equal); Methodology (equal); Software (equal); Validation (equal); Visualization (equal); Writing – original draft (equal); Writing – review & editing (equal). **Anton V. Alyanov:** Software (equal); Validation (equal); Visualization (equal).

DATA AVAILABILITY

The data that support the findings of this study are available from the corresponding author upon reasonable request.

REFERENCES

[1] D. Y. Kochkin, D. V. Zaitsev, and O. A. Kabov, "Thermocapillary rupture and contact line dynamics in the heated liquid layers," Interfacial Phenom. Heat Transfer **8**, 1–9 (2020).

[2] A. S. Mungalov, D. Y. Kochkin, I. A. Derevyannikov, and O. A. Kabov, "Free surface deformations of the horizontal liquid film heated from the substrate side, experiment and numerical simulation," Interfacial Phenom. Heat Transfer **11**, 95–107 (2023).

[3] G. I. Taylor, "Disintegration of water drops in an electric field," Proc. R. Soc. London, A **280**, 383–397 (1964).

[4] A. M. Imano and A. Beroual, "Deformation of water droplets on solid surface in electric field," J. Colloid Interf. Sci. **298**, 869–879 (2006).

[5] V. Vancauwenberghe, P. Di Marco, and D. Brutin, "Wetting and evaporation of a sessile drop under an external electric field: A review," Colloids Surf., A **432**, 50–56 (2013).

[6] L. T. Corson, C. Tsakonas, B. R. Duffy, N. J. Mottram, I. C. Sage, C. V. Brown, and S. Wilson, "Deformation of a nearly hemispherical conducting drop due to an electric field: Theory and experiment," Phys. Fluids **26**, 122106 (2014).

[7] M. Akbari and S. Mortazavi, "Three-dimensional numerical simulation of deformation of a single drop under uniform electric field," J. Appl. Fluid Mech. **10**, 693–702 (2017).

[8] A. L. Kupershtokh and D. A. Medvedev, "Dielectric droplet on a superhydrophobic substrate in an electric field," in *Proceedings of the 20th IEEE International Conference on Dielectric Liquids* (IEEE, Roma, Italy, 2019), pp. 1–4.

[9] N. M. Zubarev, "Self-similar solutions for conic cusps formation at the surface of dielectric liquids in electric field," Phys. Rev. E **65**, 055301(R) (2002).

[10] D. A. Medvedev and A. L. Kupershtokh, "Electric control of dielectric droplets and films," Phys. Fluids **33**, 122103 (2021).

[11] L. Tonks, "A theory of liquid surface rupture by a uniform electric field," Phys. Rev. **48**, 562–568 (1935).

[12] G. Lv, H. Tian, J. Shao, and D. Yu, "Pattern formation in thin polymeric films via electrohydrodynamic patterning," RSC Adv. **12**, 9681–9697 (2022).

05 October 2023 02:40:56

[13] I. Gabay, F. Paratore, E. Boyko, A. Ramos, A. D. Gat, and M. Bercovici, "Shaping liquid films by dielectrophoresis," Flow **1**, E13 (2021).

[14] A. L. Kupershtokh and D. A. Medvedev, "Perforation of thin liquid films under the action of nonuniform electric field," J. Appl. Mech. Tech. Phys. **63**, 923–930 (2022).

[15] A. L. Kupershtokh and D. A. Medvedev, "Liquid dielectric films in a nonuniform electric field: Dynamics, perforation, influence of electrode wettability," Interfacial Phenom. Heat Transfer **10**, 41–51 (2022).

[16] I. V. Marchuk, A. L. Karchevsky, A. Surtaev, and O. A. Kabov, "Heat flux at the surface of metal foil heater under evaporating sessile droplets," Int. J. Aerosp. Eng. **2015**, 391036.

[17] A. L. Karchevsky, I. V. Marchuk, and O. A. Kabov, "Calculation of the heat flux near the liquid-gas-solid contact line," Appl. Math. Modell. **40**, 1029–1037 (2016).

[18] M. J. Gibbons, C. M. Howe, P. Di Marco, and A. J. Robinson, "Local heat transfer to an evaporating sessile droplet in an electric field," J. Phys.: Conf. Ser. **745**, 032066 (2016).

[19] V. S. Ajaev and O. A. Kabov, "Heat and mass transfer near contact lines on heated surfaces," Int. J. Heat Mass Transfer **108**, 918–932 (2017).

[20] V. V. Cheverda, A. L. Karchevsky, I. V. Marchuk, and O. A. Kabov, "Heat flux density in the region of droplet contact line on a horizontal surface of a thin heated foil," Thermophys. Aeromech. **24**, 803–806 (2017).

[21] A. L. Kupershtokh, D. A. Medvedev, and A. V. Alyanov, "Simulation of substrate cooling during evaporation of pure vapor from the surface of a thin film and liquid drops," J. Appl. Ind. Math. (to be published) (2023).

[22] C. K. Aidun and J. R. Clausen, "Lattice-Boltzmann method for complex fluids," Annu. Rev. Fluid Mech. **42**, 439–472 (2010).

[23] A. L. Kupershtokh, D. A. Medvedev, and D. I. Karpov, "On equations of state in a lattice Boltzmann method," Comput. Math. Appl. **58**, 965–974 (2009).

[24] A. L. Kupershtokh, D. A. Medvedev, and I. I. Gribanov, "Thermal lattice Boltzmann method for multiphase flows," Phys. Rev. E **98**, 023308 (2018).

[25] Y. H. Qian, D. d'Humières, and P. Lallemand, "Lattice BGK models for Navier–Stokes equation," Europhys. Lett. **17**, 479–484 (1992).

[26] J. M. V. A. Koelman, "A simple lattice Boltzmann scheme for Navier–Stokes fluid flow," Europhys. Lett. **15**, 603–607 (1991).

[27] A. L. Kupershtokh, "New method of incorporating a body force term into the lattice Boltzmann equation," in *Proceedings of the 5th International EHD Workshop* (University of Poitiers, Poitiers, France, 2004), pp. 241–246.

[28] A. L. Kupershtokh, "Criterion of numerical instability of liquid state in LBE simulations," Comput. Math. Appl. **59**, 2236–2245 (2010).

[29] F. Bonaccorso, A. Montessori, A. Tiribocchi, G. Amati, M. Bernaschi, M. Lauricella, and S. Succi, "LBsoft: A parallel open-source software for simulation of colloidal systems," Comput. Phys. Commun. **256**, 107455 (2020).

[30] M. J. Krause, A. Kummerländer, S. J. Avis, H. Kusumaatmaja, D. Dapelo, F. Klemens, M. Gaedtke, N. Hafen, A. Mink, R. Trunk, J. E. Marquardt, M.-L. Maier, M. Haussmann, and S. Simonis, "OpenLB—Open source lattice Boltzmann code," Comput. Math. Appl. **81**, 258–288 (2021).

[31] M. A. Seaton and W. Smith, *DL MESO User Manual (Version 2.7, 2020)* (Daresbury Laboratory, United Kingdom, 2020).

[32] I. Ginzburg and P. M. Adler, "Boundary flow condition analysis for the three-dimensional lattice Boltzmann model," J. Phys. II France **4**, 191–214 (1994).

[33] Y. H. Qian and S. Chen, "Finite size effects in lattice-BGK models," Int. J. Mod. Phys. C **8**, 763–771 (1997).

[34] A. L. Kupershtokh, D. I. Karpov, D. A. Medvedev, C. Stamatelatos, V. P. Charalambakos, E. C. Pyrgioti, and D. P. Agoris, "Stochastic models of partial discharge activity in solid and liquid dielectrics," IET Sci. Meas. Technol. **1**, 303–311 (2007).

[35] L. D. Landau and E. M. Lifshitz, *Statistical Physics* (Elsevier Butterworth-Heinemann, Oxford, 1980).

[36] J. Hardy, O. de Pazzis, and Y. Pomeau, "Molecular dynamics of a classical lattice gas: Transport properties and time correlation functions," Phys. Rev. A **13**, 1949–1961 (1976).

[37] Q. Li, K. H. Luo, D. Q. Kang, and Q. Chen, "Contact angles in the pseudopotential lattice Boltzmann modeling of wetting," Phys. Rev. E **90**, 053301 (2014).

[38] A. L. Kupershtokh, "Contact angles in the presence of an electrical field," J. Phys.: Conf. Ser. **1675**, 012106 (2020).

[39] L. D. Landau and E. M. Lifshitz, *Electrodynamics of Continuous Media* (Pergamon Press Inc., Oxford, 1984).

05 October 2023 02:40:56